INTERNATIONAL JOURNAL FOR NUMERICAL METHODS IN FLUIDS, VOL. 5, 245–255 (1985)

A NUMERICAL PROCEDURE FOR THE GENERATION OF ORTHOGONAL BODY-FITTED CO-ORDINATE SYSTEMS WITH DIRECT DETERMINATION OF GRID POINTS ON THE BOUNDARY

DIMITRIS E. PAPANTONIS* AND NICHOLAS A. ATHANASSIADIS†

Department of Mechanical Engineering, National Technical University of Athens, 42 October 28 Avenue Athens, Greece

SUMMARY

The procedure proposed is based on the solution by finite difference means of a set of Laplace's equations, by the application of a relaxation method.

The curvilinear orthogonal grid so generated is fitted to a 2-D physical domain with closed boundary and the contribution of the present work consists in the arbitrary choice of grid points on two adjacent boundaries, in order to achieve the desired density of grid points where the geometry of the boundaries varies rapidly.

The method proposed is rapid and stable. Some characteristic examples are finally presented.

KEY WORDS Orthogonal Body-Fitted Grid

INTRODUCTION

In recent years considerable work has been reported on the generation of body- or boundary-fitted curvilinear co-ordinate systems, the great advantage of which is the easy and accurate description of boundary conditions in the case of complex geometries. In some cases it is desirable that the body-fitted curvilinear co-ordinate system also be orthogonal because of the simplicity such a system offers in the expression of differential equations.

The existing methods for the generation of a curvilinear body-fitted co-ordinate system are based on two different principles: conformal mapping and the solution of differential equations of elliptic type. Our interest will be principally focused on the second case where one can distinguish two possibilities; to take the natural co-ordinates to be solutions of Laplace's equations in the physical domain[1] or to reverse this procedure by taking the physical co-ordinates to be solutions in the transformed plane of a linear elliptic system.[2–4]

Thompson *et al.*[5] describe a general method for the generation of non-dimensional co-ordinate systems in which the location of mesh lines can be controlled by the use of 'packing' functions to accommodate rapid variations of the field. In their work the natural co-ordinates were considered as solutions of an elliptic differential system in the physical plane; their method was also extended to multiconnected regions.

Potter and Tuttle[6] and Davies[7] have developed numerical procedures for the orthogonalization

*Lecturer
†Professor

0271–2091/85/03 0245–11$01.10

Received 9 January 1984
Revised 6 April 1984

of a discrete non-orthogonal 2-D co-ordinate system, preserving one set of the non-orthogonal co-ordinate lines.

Work on orthogonal or non-orthogonal curvilinear body-fitted systems is also reported with some possibilities for controlling the distribution of mesh lines by the introduction of forcing or weighting functions or of source terms or of a scaling constant.[8-14] In these cases, and especially in the case of orthogonal curvilinear systems, with the proposed methods it is not possible to arbitrarily choose the grid points on the boundaries.

Our task was to generate a curvilinear orthogonal 2-D co-ordinate system with arbitrarily chosen grid points on two adjacent boundaries. As in most of the cases the geometry of one or two of the boundaries changes rapidly and on the others the geometry changes smoothly, with this method, the grid obtained is generally very satisfactory.

Another advantage of this method is that it can also be applied in the case of external flows by dividing the domain into two subdomains and finally matching the two subgrids obtained, as is also performed by Tatum.[15] This method can also be applied to multiconnected regions.

THEORETICAL BASIS—FINITE-DIFFERENCE EQUATIONS

Let (x, y) be the Cartesian co-ordinate system in the physical 2-D domain and (ξ, η) the desired orthogonal curvilinear system; the set of lines $\xi = \text{constant}$ and $\eta = \text{constant}$ form a grid which must be orthogonal in the physical plane. It is known that the solution of a set of Laplace's equations in the physical domain (x, y):

$$\nabla^2\phi = 0 \Rightarrow \frac{\partial^2\phi}{\partial x^2} + \frac{\partial^2\phi}{\partial y^2} = 0 \tag{1}$$

and

$$\nabla^2\psi = 0 \Rightarrow \frac{\partial^2\psi}{\partial x^2} + \frac{\partial^2\psi}{\partial y^2} = 0 \tag{2}$$

corresponds to a set of $\phi = \text{constant}$ and $\psi = \text{constant}$ lines which are everywhere orthogonal between them. If we replace the ϕ parameter by ξ and the ψ by η, it is clear that by solving the Laplace's equations (1) and (2) the desired curvilinear orthogonal grid is produced; this means that the $\xi = \xi(x, y) = \text{constant}$ and $\eta = \eta(x, y) = \text{constant}$ lines are orthogonal between them. Also by taking the physical boundaries of the domain (x, y) as solutions of the equations (1) and (2), the so generated orthogonal curvilinear system is body- or boundary-fitted.

Expressing the physical co-ordinates x and y as functions of the ξ and η, i.e. $x = x(\xi, \eta)$ and $y = y(\xi, \eta)$, the above Laplace's equations (1) and (2), taking into account the orthogonality of the $\xi = \text{constant}$ and $\eta = \text{constant}$ lines, are equivalent to the Laplace's equations:

$$\frac{\partial^2 x}{\partial \xi^2} + \frac{\partial^2 x}{\partial \eta^2} = 0 \tag{3}$$

$$\frac{\partial^2 y}{\partial \xi^2} + \frac{\partial^2 y}{\partial \eta^2} = 0 \tag{4}$$

The set of equations (3) and (4) is equivalent to the set (1) and (2), taking into account the orthogonality conditions of the $\xi = \text{constant}$ and $\eta = \text{constant}$ lines.

Introducing a scaling factor h in the set of Laplace's equations (3) and (4) which is equal to the ratio of the scale factors h_ξ and h_η associated with the orthogonal co-ordinates ξ and η, respectively,

the following set of equations is obtained:

$$\frac{\partial^2 x}{\partial \xi^2} + \frac{\partial^2 x}{h^2 \partial \eta^2} = 0 \tag{3'}$$

$$\frac{\partial^2 y}{\partial \xi^2} + \frac{\partial^2 y}{h^2 \partial \eta^2} = 0 \tag{4'}$$

For different values of the h factor, an infinity of curvilinear orthogonal grids can be generated for a specified physical domain. As is developed in Reference 9, integrating the equations (3') over control volumes centred on the $\xi - \eta$ grid points, the following finite-difference equation is obtained:

$$A_P X_P = A_E X_E + A_W X_W + A_S X_S + A_N X_N \tag{5}$$

where the grid points in the (x, y) domain, surrounding the grid-point P, are characterized by the subscripts E, W, N and S, with

$$A_E = \frac{1}{(\xi_E - \xi_W)(\xi_E - \xi_P)} \qquad A_W = \frac{1}{(\xi_E - \xi_W)(\xi_P - \xi_W)}$$

$$A_N = \frac{1}{(\eta_N - \eta_S)(\eta_N - \eta_P)h^2} \qquad A_S = \frac{1}{(\eta_N - \eta_S)(\eta_P - \eta_S)h^2}$$

$$A_P = A_E + A_W + A_N + A_S$$

From the differential equation (4'), governing the Y location of the grid-points, applying the same procedure, the following similar finite-difference equation is obtained:

$$A_P Y_P = A_E Y_E + A_W Y_W + A_N Y_N + A_S Y_S \tag{6}$$

The finite-difference equations (5) and (6) are solved numerically by applying an iterative relaxation method with the appropriate boundary conditions, starting from an initial guess for the solution.

BOUNDARY CONDITIONS—INITIAL SOLUTION

The physical boundaries of the (x, y) domain must be grid lines; this means that every pair of opposite boundaries corresponds to a $\xi =$ constant or $\eta =$ constant value (Dirichlet boundary conditions). For simplicity, as is seen in Figure 1 the value $\eta = 0$ is associated with the boundary AB the value $\eta = 1$ is associated with DC, the value $\xi = 0$ is associated with AD and the value $\xi = 1$ is associated with BC.

A restriction is already apparent; the boundaries of the physical domain must, as solutions of Laplace's equations, be perpendicular between them at the junction points A, B, C and D (Figure 1). In some cases this restriction can be easily accomplished, if it is not initially, by extending the domain with a fictitious boundary which would be perpendicular to the adjacent boundaries.

Up to this point the same procedure has been adopted as in previous work.[9,11] The principal difference between the earlier work and the proposed procedure is that previously the $\xi =$ constant and $\eta =$ constant lines have had a predetermined set of values and in the present case the final ξ and η values are obtained by the numerical procedure.

As is evident, one grid point on the boundary, the intersection of a $\xi = \xi_1$ line with the boundary, cannot be previously known. By the use of 'forcing' or 'packing' functions[8,11] it is possible to control the density of grid points, but again the grid points are not precisely predetermined on any one of the boundaries.

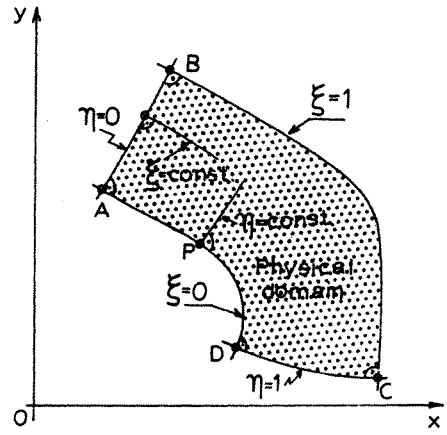

Figure 1. Definition of physical domain

In the present work our task is to find the ξ (and/or the η) values of the ξ = constant (and/or η-constant) lines which start from arbitrarily chosen points on one of the opposite boundaries (AD of Figure 1).

The corresponding grid point on the opposite boundary (BC in our case) will be obtained from the numerical solution of the problem, which means that they are not previously known. The same procedure can be applied to the adjacent boundaries, that is to choose arbitrarily the grid points on one of them (AB or CD of Figure 1). Referring to Figure 1, a number of grid points P can be arbitrarily chosen on the boundary AD and the corresponding values of $\eta = \eta_1$ will be determined.

NUMERICAL PROCEDURE

The numerical procedure must start from an initial solution, i.e. an initial guess for the physical co-ordinates (x, y) of the grid-points and an initial distribution of the ξ and η values. It is evident that the arbitrarily chosen grid points on the adjacent boundary (say on the AD boundary of Figures 1 and 2) must also be points of the initial solution.

Suppose that we wish to obtain the η = constant lines starting from arbitrarily chosen points on the boundary AD ($I = 1$, Figure 2). These lines have, at the beginning of the procedure, an initial guess for the η values which in general is not the correct one (for the $J = 1$ boundary a similar procedure is followed for the ξ = constant lines).

The grid points $(2, J)$ must normally be located at the normals to the boundary from the corresponding $(1, J)$ points. Therefore for the next iteration the new grid points $(2, J)$ (points $P_v(2, J)$ on Figure 2) are taken as the intersection point of the previous $I = 2$ line (taken as a cubic spline) with the normals to the boundary from the fixed $(1, J)$ points.

The grid points on the opposite boundary (the line $I = \mathrm{NI}$ in Figure 2) are taken as the intersection points of the boundary with the normals to the boundary from the points $(\mathrm{NI} = 1, J)$ (Figure 2).

The finite-difference equations (5) and (6) are solved for all the internal nodes of the grid (for $I = 2$ to $I = \mathrm{NI} - \mathrm{I}$ and for $J = 2$ to $J = \mathrm{NJ} - 1$). The new physical co-ordinates X_p and Y_p of the grid points are then obtained. As the η (and/or the ξ) values are not necessarily the correct ones, the co-ordinates (x, y) obtained for the grid points of the $I = 2$ line are not on the normals to the boundary from the corresponding points, as they would be if the η value was the correct one. This can be expressed by the fact that the inclination of the $(1, J)$, $(2, J)$ segment is not the same as that of the

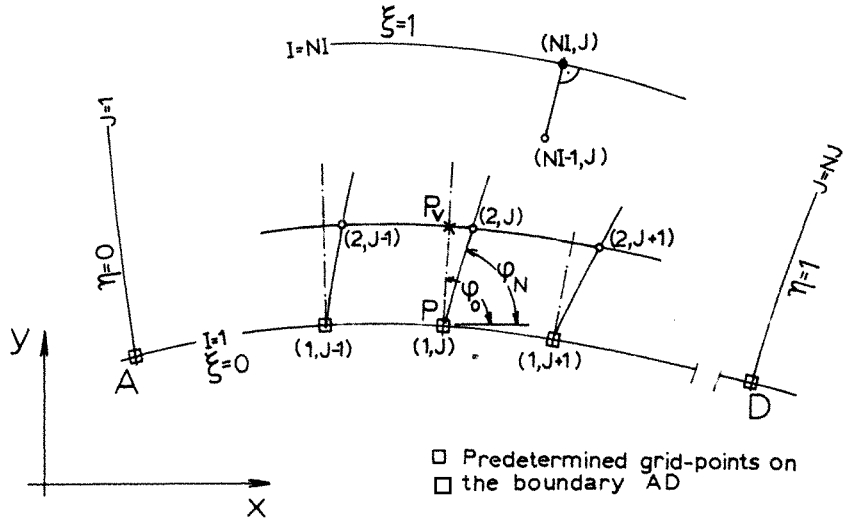

Figure 2. Definition of the boundary conditions

normal, which means that the angle φ_N is not equal to the angle φ_0 of the normal (as in Figure 2, the angles are taken with respect to the horizontal direction). The correction to the η value is taken proportional to the difference $\delta\varphi(J) = \varphi_0(J) - \varphi_N(J)$.

In our examples we take:

$$\delta\eta(J) = C_1 \delta\varphi(J) \tag{7}$$

with $\delta\varphi$ in radians and C_1 the proportionality factor which was taken as $C_1 = 0{\cdot}0005C$ with $C \geqslant 1$. The influence of the C value on the procedure is commented on in the last paragraph of the examples section.

The new value of η_N of the $\eta(J) = \text{constant}$ line is then obtained from its previous value $\eta_0(J)$ using the relation

$$\eta_N(J) = \eta_0(J) - \delta\eta(J) \tag{8}$$

The minus sign is justified by the remark that if the η-values corresponding to a grid point and to the points surrounding it are, say, greater than the correct ones, the point $(2, J)$ in Figure 2, taken by the finite-difference equations, will normally be located to the right of the normal, near the boundary which corresponds to the value $\eta = 1$, which means that $(\varphi_0(J) - \varphi_N(J)) > 0$ (as is shown in Figure 2).

For the test of convergence it is required that the maximum value of all the $\delta\varphi(J)$ is less than a prespecified small number. In our examples it is taken as

$$\max\,[\delta\varphi(J)] \leqslant 1{\cdot}6 \times 10^{-2}\ \text{rad} \simeq 0{\cdot}9^0 = \delta\varphi_{\min}$$

The convergence of the X_p and Y_p co-ordinates is a result of the convergence of the η (and ξ) values, and as the deviation $\delta\eta$ diminishes the δX_p and δY_p deviations also diminish. In the examples presented the maximum deviation δX_p and δY_p at the end of the solution was of the order of $\delta X_p \simeq 0{\cdot}0018L$, where L is the maximum dimension of the domain of interest.

COMPUTATIONAL DETAILS

In the case of points of discontinuity on the boundaries we have to distinguish two cases; the discontinuity is on the boundary with the arbitrarily chosen grid points or on the opposite

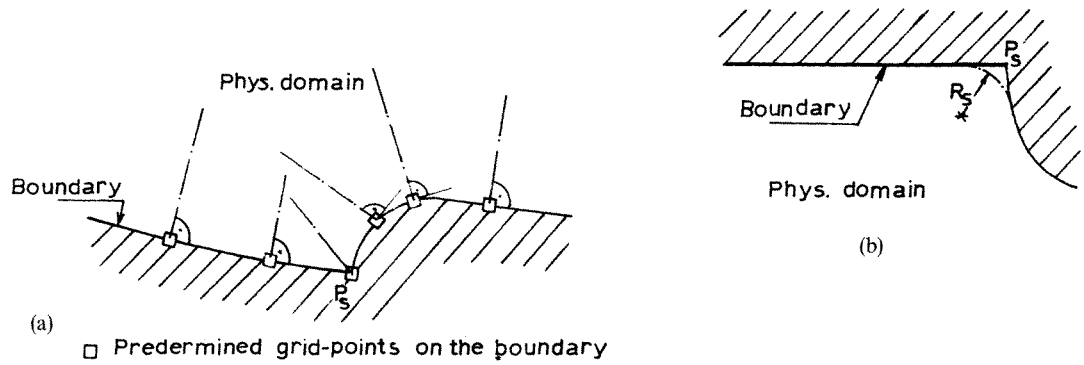

Figure 3. Boundary conditions in discontinuity points: (a) on the boundary where the grid-points are predetermined; (b) on the opposite boundary

boundary. In the first case (Figure 3(a)) the η-line (or ξ-line) must leave the boundary at the discontinuity point P_s by the bisectrix of the two tangents (this is equivalent to the $\phi = \text{constant}$ lines in the singular points of potential flow).

In the second case (Figure 3(b)) the boundary is smoothed by fitting a circle of radius R_s tangent to it on both sides of discontinuity point P_s. This procedure was proposed by Antonopoulos,[9] who found that an optimum value of R_s is $0{\cdot}05L$. In our examples the value of R_s was taken of the order of $0{\cdot}0125L$.

As far as the initial co-ordinates (X_p, Y_p) of the grid points are concerned, the following simple method was employed: from the fixed chosen points on the boundary lines were drawn straight lines. These lines were divided into (NI − I) segments, the last point being on the opposite boundary.

The initial guess of the values of the $\xi = \text{constant}$ and $\eta = \text{constant}$ lines was chosen arbitrarily also between the limit values 0 and 1, making a reasonable distribution according to the case.

In the examples presented here, with the initial guesses for the (X_p, Y_p) co-ordinates and the ξ and η values, at the beginning of the calculations the maximum deviation $\delta\varphi$ was of the order of even 70° and the maximum deviation δX_p, δY_p was of the order of $0{\cdot}05L$. This proves that no special attention was paid to the initial guess for the solution.

The factor h was calculated as proposed by Antonopoulos,[9] that is

$$h = \frac{L_\xi}{L_\eta}$$

where L_ξ is the total length of all the $\xi = \text{constant}$ lines and L_η is the total length of all the $\eta = \text{constant}$ lines. In the examples presented, after a number of iterations the changes of h value were small and the h value was not recalculated any more.

EXAMPLES

To illustrate the capabilities of the proposed method for the body-fitted orthogonal curvilinear, three characteristic examples are presented.

In the first a 2-D channel is concerned and Figure 4(a) shows the initial guess of the solution. The values of constant lines were first taken by equally dividing the space between 0 and 1. In Figure 4(b) is shown the solution obtained for the curvilinear (21 × 21) grid, with the final values of the $\eta = \text{constant}$ lines. In order to test the method the initial guess of the η values was taken with all

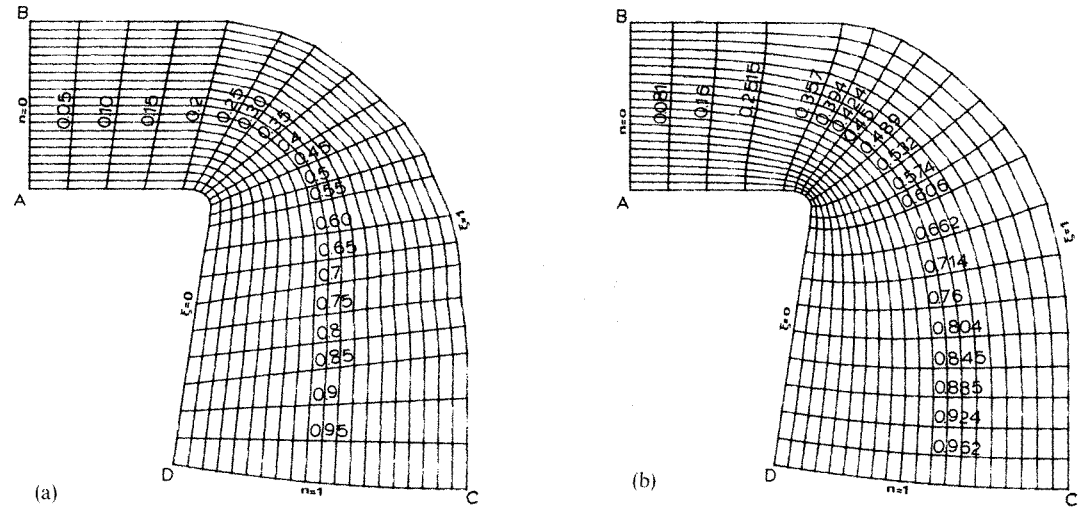

Figure 4. (21 × 21) grid generation into a curved channel: (a) initial solution; (b) obtained orthogonal curvilinear grid

the η values bigger than those resulting from the first run of the program. The result is very satisfactory, as the bigger fractional change of all the η values between the two runs was of the order of 3 per cent. The grid points obtained from the two different runs of the program were practically identical. The grid points on the boundaries AD and AB were predetermined.

In Figure 5(a) is shown the initial solution for the grid in the blade-to-blade domain of a turbomachine and in Figure 5(b) the curvilinear orthogonal (33 × 21) grid obtained. In this case the grid points on the boundaries AB and AD were predetermined. It can be pointed out that the obtained distribution of grid points on the boundary opposite to AB, i.e. the boundary BC, is not the desirable one because of the abrupt change of geometry of the boundary BC too.

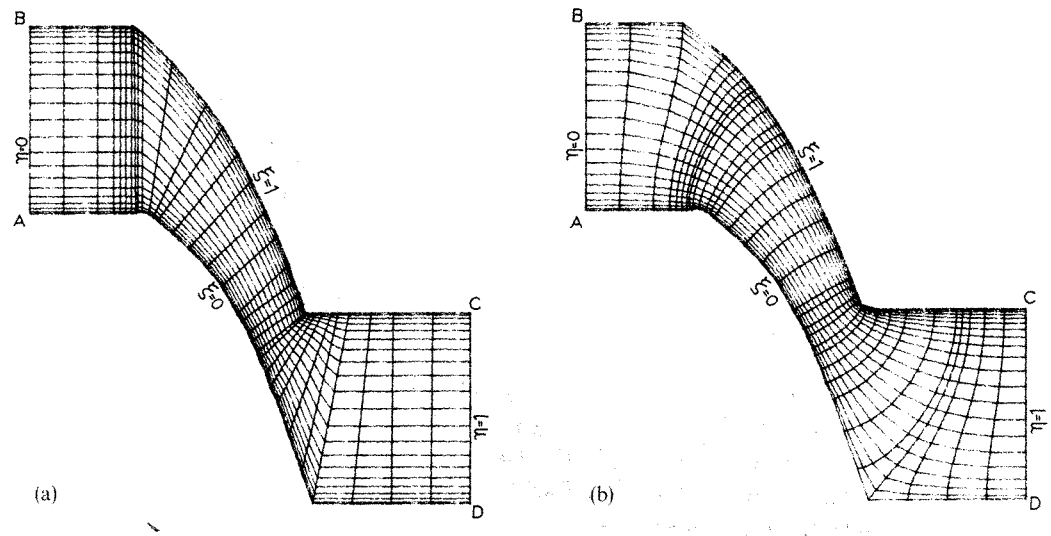

Figure 5. (33 × 21) grid generation in a blade-to-blade domain; (a) initial solution; (b) obtained orthogonal curvilinear grid

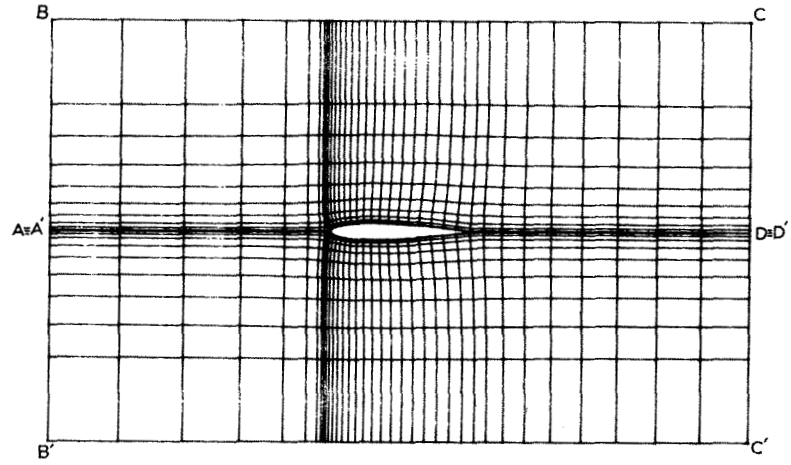

Figure 6. (37 × 42) orthogonal curvilinear grid around a NACA-0012 wing section with zero angle of incidence

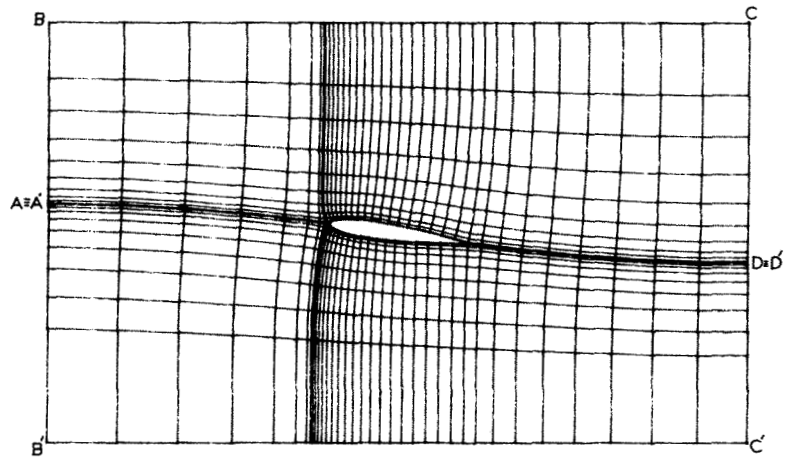

Figure 7. (37 × 42) orthogonal curvilinear grid around a NACA-0012 wing section with 8° angle of incidence

In Figure 6 is shown the (37 × 42) grid obtained around a NACA-0012 wing section with zero angle of incidence. This grid is the result of the superposition, as explained in the introduction, of two subgrids; one containing the upper boundary of the wing section and the other containing its lower boundary. As was expected, the two grids are symmetrical about the axis of symmetry. In Figure 7 is shown the grid obtained with an angle of incidence equal to 8° and Figure 8 is an amplification of this grid around the leading edge of the wing section.

The two subdomains are obtained by extending the chord of the wing section by two parabolas, one from the leading edge to the front boundary and the other from the trailing edge to the rear boundary.

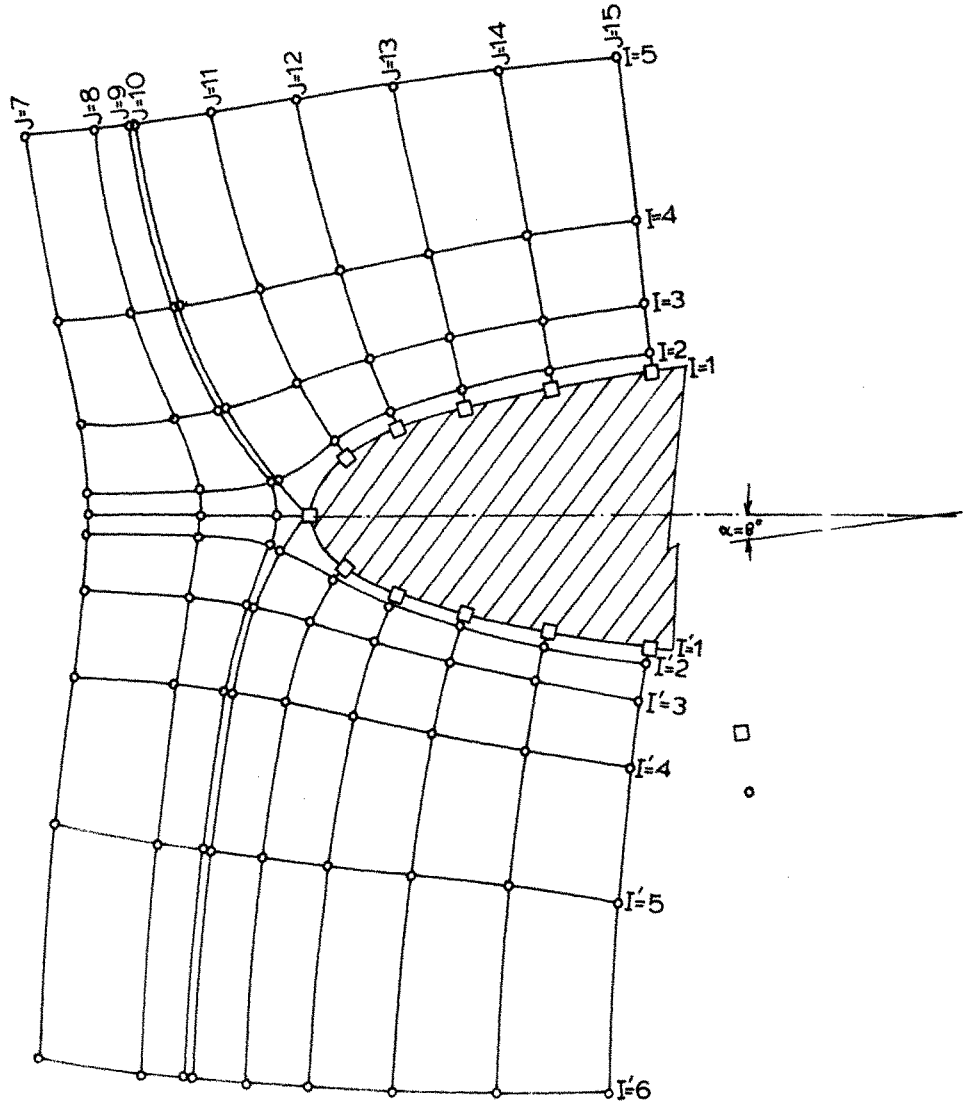

Figure 8. Amplification of the (37 × 42) grid around the leading edge of the NACA-0012 wing section with 8° angle of incidence

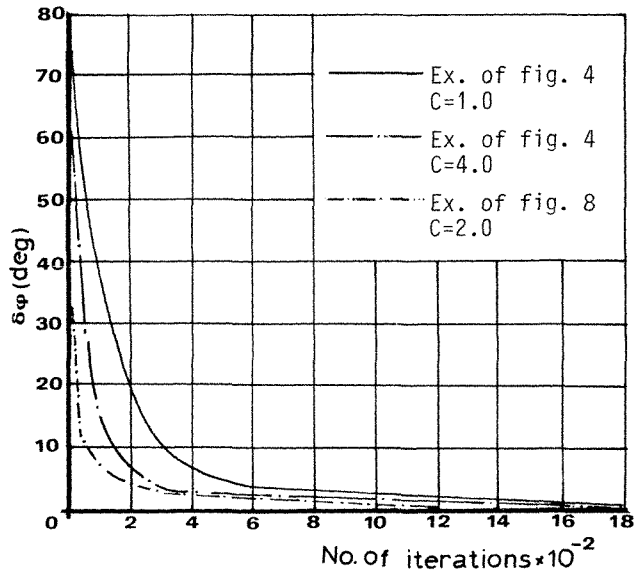

Figure 9. Speed of convergence for the examples presented

In Figure 9 is drawn the change of the maximum $\delta\varphi$ deviation with the number of iterations obtained in the case of the presented examples. The C coefficient of the relation (7) was taken equal to the value marked as parameter for $\max(\delta\varphi) > C\delta\varphi_{\min}$, and equal to 1 ($C = 1$) for $\max(\delta\varphi) < C\delta\varphi_{\min}$. From these curves the following remark comes out; with a greater value of C the initial speed of convergence is greater, but ultimately the shortening of the run-time is not important; however, an important value of C can provoke instability of the procedure (the change $\delta\eta(J)$ must not be greater than the difference $\eta(J) - \eta(J-1)$, or $\eta(J) - \eta(J+1)$).

CONCLUSION

From the examples presented, it is proved that the proposed method is a general method for the generation of 2-D body fitted curvilinear orthogonal grids. The results are satisfactory even with rapidly varying density of the arbitrary grid-points on the boundary or near to points of discontinuity.

LIST OF SYMBOLS

x, y	Cartesian co-ordinates in the natural domain
ϕ	Potential function
ψ	Stream function
ξ, η	Values of the grid lines
h	Scaling factor
A	Coefficients of the finite-difference equations
I	Number of the $\xi =$ constant lines
J	Number of the $\eta =$ constant lines
φ_0	Angle of the vertical to the boundary from a predetermined grid point with respect to the horizontal direction.

φ_N	Angle of the actual segment of the grid with respect to the horizontal direction.
$\delta\varphi = \varphi_0 - \varphi_N$	Angular deviation
C	Acceleration factor
δx	Deviation of the x-co-ordinate of a grid point between two iterations
δy	Deviation of the y-co-ordinate of a grid point between two iterations
R_s	Smoothing radius of the boundary at the discontinuity point
L	Maximum dimension of the physical domain
L_ξ	Total length of all $\xi =$ constant lines
L_η	Total length of all $\eta =$ constant lines

REFERENCES

1. A. M. Winslow, 'Numerical solution of the quasilinear poisson equation in a nonuniform triangle mesh', *J. Comp. Phys.*, **2,** 149–172 (1967).
2. W. B. Barfield, 'Numerical method for generating orthogonal curvilinear meshes', *J. Comp. Phys*, **5,** 23–33 (1970).
3. W. B. Barfield, 'An optimal mesh generator for Lagrangian hydrodynamic calculations in two space dimensions', *J. Comp. Phys.*, **6,** 417–429 (1970).
4. A. A. Amsden and C. W. Hirt, 'A simple scheme for generating general curvilinear grids', *J. Comp. Phys.*, **11,** 348–359 (1973).
5. J. E. Thompson, F. C. Thames, C. W. Mastin, 'Automatic numerical generation of body-fitted curvilinear coordinate system for field containing any number of arbitrary two-dimensional bodies', *J. Comp. Phys.*, **15,** 299–319 (1974).
6. D. E. Potter and G. H. Tuttle, 'The construction of discrete orthogonal coordinates', *J. Comp. Phys.*, **13,** 483–501 (1973).
7. C. W. Davies, 'An initial value approach to the prediction of discrete orthogonal coordinates', *J. Comp. Phys.*, **39,** 164–178 (1981).
8. T. K. Hung and T. D. Brown, 'An implicit finite difference Method for Solving the Navier–Stokes equation using orthogonal curvilinear coordinates', *J. Comp. Phys.*, **23,** 343–363 (1977).
9. K. A. Antonopoulos, 'Prediction of flow and heat transfer in rod bubbles', *Ph.D. Thesis*, Imperial College, 1979.
10. R. Camarero and M. Younis, 'Efficient generation of body-fitted coordinates for cascades using multigrid', *AIAA Journal*, **18,** (5), 487 (1980).
11. P. D. Thomas and J. F. Middlecoff, 'Direct control of the grid point distribution in meshes generated by elliptic equations', *AIAA Journal*, **18,** (6), 652 (1980).
12. C. D. Mobley and R. J. Stewart, 'Note on the numerical generation of boundary-fitted orthogonal curvilinear coordinate system', *J. Comp. Phys.*, **34,** 124–135 (1980).
13. C. Farell and J. Adamczyk, 'Full potential solution of transonic quasi-three-dimensional flow through a cascade using artificial compressibility', *Trans. ASME, J. Eng. for Power*, **104,** 143 (1982).
14. M. Visbal and D. Knight, 'Generation of orthogonal or nearly orthogonal coordinates with grid control near boundaries', *AIAA Journal*, **20,** (3), 305 (1982).
15. K. E. Tatum, 'Finite element method for transonic flow analysis', *AIAA Journal*, **21,** (8), 1071 (1983).
16. M. E. Younis and R. Camarero, 'Finite volume method for blade-to-blade flows using a body-fitted mesh', *AIAA Journal*, **19,** (1), 1500 (1981).